PHYSICAL REVIEW C, VOLUME 61, 034004

Charge symmetry breaking in neutron matter

Aya Ishihara,[1,*] Akira Suzuki,[1] Masahiro Kimura,[2] and Katsuhiko Suzuki[3,†]
[1]*Department of Physics, Science University of Tokyo, Shinjuku, Tokyo, Japan*
[2]*Department of Electronics Engineering, Suwa College, Chino, Nagano, Japan*
[3]*Physik Department, Technische Universität München, D-85747 Garching, Germany*
(Received 4 February 1999; published 16 February 2000)

We examine the nuclear medium effect on the charge symmetry breaking (CSB) caused by isospin mixing of two neutral vector mesons interacting with nucleons in neutron matter. It is found that isospin mixing is strongly enhanced in neutron matter as the neutron density increases and the charge symmetry is broken to a large extent. We illustrate the influence of the enhanced CSB for bulk quantities by calculating the mass of a fictitious neutron star composed of only neutrons. For the stars with central densities around the normal density of nuclear matter, the masses are reduced by as much as 35% in comparison with those emerging from an ordinary relativistic nuclear model with no CSB considered. The effect of CSB is attenuated for stars with higher central densities which actual neutron stars are supposed to have, although the charge symmetry remains broken to a large extent.

PACS number(s): 21.30.−x, 21.65.+f, 24.10.Jv, 26.60.+c

I. INTRODUCTION

Charge symmetry is one of the salient features of nuclear forces. However, it is known that the symmetry is slightly broken and only approximate [1]. A typical manifestation of charge symmetry breaking (CSB) is seen in the small difference between the *nn* and *pp* scattering lengths that remains after the Coulomb correction is made [2–4]. A part of the mass difference between ^{3}H and ^{3}He is another example that could be understood in terms of CSB [5–7].

It has been suggested that the CSB caused by isospin mixing of two neutral vector mesons can account for most of the difference between the *pp* and *nn* scattering lengths [7,8]. Piekarewicz and Williams proposed a basic mechanism for the isospin mixing of vector mesons [9]. According to this, two vector mesons in different isospin eigenstates undertake a transition to each other through a baryon loop. An essential point is the incomplete cancellation between the contributions from a loop with a proton and antiproton and one with a neutron and antineutron to the transition amplitude. The small mass difference between the proton and neutron causes this incomplete cancellation. One can take advantage of this idea to study the nuclear medium effect on CSB. The medium effect on the isospin mixing appears through the Pauli principle for nucleons in the intermediate baryon loops and nucleon effective masses, leading to a density-dependent CSB (DDCSB) in a nuclear medium.

With the above idea of DDCSB, we have examined the medium effect on the isospin mixing in nuclear matter in a previous work [10]. We found that the density dependence of CSB works in the right direction such that the Okamoto-Nolen-Schiffer anomaly is resolved [5,11]. A striking feature which we have learned there is that the isospin mixing is rapidly and strongly enhanced as soon as nuclear matter departs from the isosymmetric state. The strong isospin mixing induces a large energy increase of nuclear matter and works eventually to restore minimal isospin symmetry. This motivated us to investigate the medium effect on CSB in neutron matter which has the largest isospin asymmetry. We will pursue it in this paper.

The extent of the isospin mixing is usually parametrized in terms of a mixing angle, which can depend on the nucleon density of the medium. We are mainly interested in (i) the nuclear density dependence of the mixing angle and (ii) the influence of DDCSB due to the isospin mixing on the equation of state of neutron matter. Regarding the latter, we illustrate it by calculating the mass of a fictitious neutron star composed of only neutrons, since the equation of state is substantial to determine the mass.

In our previous works, we have used a relativistic nuclear model proposed by Zimanyi and Moszkowski (ZM) [12]. This is a modified version of quantum hadrodynamic nuclear models originally proposed by Walecka [13], and can reproduce the compression modulus as well as the correct saturation density and binding energy per nucleon of nuclear matter. However, when the model by ZM is applied to neutron matter, we find that it makes the equation of state in the high density region so soft that a type of gas-liquid phase transition can take place. In other words, the attractive interaction between the nucleon and scalar meson seems to be too strong in the model by ZM in the high density region. Since our purpose in the present work is to investigate how much CSB is modified in isospin asymmetric matter, we make use of an original version called QHD II of quantum hadrodynamic nuclear models rather than using the model by ZM. We modify it such that the model can describe the transition between two vector mesons. We refer to QHD II whenever we compare our results with those from ordinary nuclear models with no CSB considered [13].

We arrange this paper as follows. In the next section, we present the modified QHD II as our theoretical framework for the study of CSB in neutron matter. In Sec. III, we de-

*Present address: Department of Physics, University of Texas at Austin, Austin, TX.

†Present address: Theory Group, RCNP, Osaka University, Ibaraki, Osaka, Japan.

0556-2813/2000/61(3)/034004(9)/$15.00

scribe the transition process of vector mesons in detail and relate the transition amplitude to the isospin mixing angle in neutron matter. We demonstrate DDCSB on various quantities in Sec. IV. A discussion and comments are also given there.

II. QHD II WITH BROKEN ISOSPIN SYMMETRY

The version QHD II of the quantum hadrodynamic nuclear models proposed by Walecka contains an isovector-vector meson degree of freedom in addition to an isoscalar-scalar and isoscalar-vector mesons which are relevant degrees of freedom in QHD I [13]. The Lagrangian of QHD II is given by

$$\mathcal{L}_{QHD\ \ II}=\bar{\Psi}\left[\gamma^{\mu}(i\partial_{\mu}-G_0V^{(0)}_{\mu}-G_1\tau_3V^{(1)}_{\mu}) -F_1\left(\frac{\sigma^{\mu\nu}}{2M_N}\right)\tau_3\partial_{\mu}V^{(1)}_{\nu}-(M-f\phi)\right]\Psi +\frac{1}{2}(\partial^{\mu}\phi\partial_{\mu}\phi-m_{\sigma}^2\phi^2)+\sum_{I=0}^{1}\times\left[-\frac{1}{4}F^{(I)\mu\nu}F^{(I)}_{\mu\nu}+\frac{1}{2}m_I^2V^{(I)\mu}V^{(I)}_{\mu}\right], \tag{1}$$

where Ψ is the nucleon field operator which is a spinor in isospin space and can be expressed as

$$\Psi(\boldsymbol{x})=\begin{pmatrix}\Psi_p(\boldsymbol{x})\\ \Psi_n(\boldsymbol{x})\end{pmatrix}, \tag{2}$$

with the field operators for the proton (p) and neutron (n) as the upper and lower components, respectively; τ_3 is the third component of the Pauli's isospin matrices, and $\sigma^{\mu\nu}=(i/2)[\gamma^{\mu},\gamma^{\nu}]$. Regarding mesons involved in Eq. (1), ϕ, $V^{(0)}$, and $V^{(1)}$ are the field operators for the isoscalar-scalar, isoscalar-vector, and neutral isovector-vector mesons, respectively, m_{σ}, m_0, and m_1 are their masses, f, G_0, G_1, and F_1 their coupling constants with nucleon, and $F^{(I)\mu\nu}$ the tensor fields of vector mesons defined by

$$F^{(I)\mu\nu}=\partial^{\mu}V^{(I)\nu}-\partial^{\nu}V^{(I)\mu}, \tag{3}$$

where the superscript I denotes the isospin and takes 0 or 1. The parameter M_N in Eq. (1) is the average of the proton and neutron masses. We follow the metric convention of Bjorken and Drell [14]. The diagonal ''mass'' matrix M has proton mass (M_p) and neutron mass (M_n) as its diagonal elements. Since the tensor coupling of the isoscalar-vector meson with the nucleon is expected to be negligibly small, we ignored it [15]. We will shortly apply the mean-field approximation (MFA) in which all meson fields are replaced by classical fields. The isovector meson does not play any relevant roles in the MFA for isosymmetric nuclear matter, since the corresponding classical field is proportional to the nucleon isovector density as we will see later. However, it becomes important in isospin *asymmetric* nuclear matter such as neutron matter in our case.

We add a phenomenological interaction which causes the transition between the isoscalar- and isovector-vector mesons to the model of QHD II. We assume the form of the interaction to be

$$\mathcal{L}_X=\epsilon(n)V^{(0)}_{\mu}V^{(1)\mu}. \tag{4}$$

The $\epsilon(n)$ is related to the isospin mixing that is dictated by the transition between the vector mesons and can depend on the neutron number density n. We will relate $\epsilon(n)$ to the transition amplitude in the next section. The Lagrangian with which we start our study of neutron matter is, thus,

$$\mathcal{L}=\mathcal{L}_{QHD\ \ II}+\mathcal{L}_X. \tag{5}$$

Owing to $\mathcal{L}_X$, the vector mesons are no longer in isospin eigenstates, but mixtures of them. Nuclear systems in which nucleons exchange such mesons eventually break the charge symmetry.

Let us apply the mean-field approximation to our study of neutron matter. Many authors have discussed the validity of the MFA in the quantum hadrodynamic nuclear model and found it to be a good approximation for a first step to study many-nucleon systems in the relativistic scheme [13]. Although the quantum correction is considered to improve the approximation, we leave it out for simplicity [16]. In a static and uniform state, all meson fields in Eq. (5) are replaced by constant classical fields in the MFA according to

$$\phi\rightarrow\langle\phi\rangle\equiv\phi_c, \tag{6}$$

$$V^{(I)}_{\mu}\rightarrow\langle V^{(I)}_{\mu}\rangle\equiv\delta_{\mu 0}V^{(I)}_c, \tag{7}$$

for $I=0$ and 1, where $\langle\cdots\rangle$ represents the expectation value of a quantity inside the brackets in the ground state of neutron matter. The Lagrangian in the MFA is, then,

$$\mathcal{L}_{MFT}=\bar{\Psi}[i\gamma^{\mu}\partial_{\mu}-G_0\gamma^0V^{(0)}_c-G_1\gamma^0\tau_3V^{(1)}_c-M^*(\phi_c)]\Psi -\frac{1}{2}[m_{\sigma}^2\phi_c^2-m_0^2V^{(0)2}_c-m_1^2V^{(1)2}_c]+\epsilon(n)V^{(0)}_cV^{(1)}_c. \tag{8}$$

The elements of the diagonal effective mass matrix $M^*(\phi_c)$ are

$$M^*_b(\phi_c)=M_b-f\phi_c, \tag{9}$$

where b stands for p or n. Note that the tensor coupling term of the isovector-vector meson plays no role in the MFA for static and uniform matter.

The vector meson sector in $\mathcal{L}_{MFT}$ can be diagonalized in terms of

$$\omega_c=V^{(0)}_c\cos\theta-V^{(1)}_c\sin\theta, \tag{10}$$

$$\rho_c=V^{(0)}_c\sin\theta+V^{(1)}_c\cos\theta. \tag{11}$$

The ω_c and ρ_c may be interpreted as the classical fields of *physical* vector mesons ω and ρ^0 whose dominant components have $I=0$ and 1, respectively. The diagonalization condition determines the mixing angle θ to be

$$\tan 2\theta=\frac{2\epsilon(n)}{m_1^2-m_0^2}. \tag{12}$$

Remember that θ depends on the neutron density through $\epsilon(n)$. The diagonalized Lagrangian is written as

$$\mathcal{L}_{MFT}=\bar{\Psi}[i\gamma^\mu\partial_\mu-g\gamma^0\omega_c-g'\gamma^0\tau_3\rho_c-M^*(\phi_c)]\Psi -\frac{1}{2}(m_\sigma^2\phi_c^2-m_\omega^2\omega_c^2-m_\rho^2\rho_c^2), \tag{13}$$

where

$$g=\begin{pmatrix} g_p & 0\\ 0 & g_n\end{pmatrix}=\begin{pmatrix} G_0\cos\theta-G_1\sin\theta & 0\\ 0 & G_0\cos\theta+G_1\sin\theta\end{pmatrix}, \tag{14}$$

$$g'=\begin{pmatrix} g'_p & 0\\ 0 & g'_n\end{pmatrix}=\begin{pmatrix} G_1\cos\theta+G_0\sin\theta & 0\\ 0 & G_1\cos\theta-G_0\sin\theta\end{pmatrix}. \tag{15}$$

The masses m_ω and m_ρ, which are defined by

$$m_\omega^2=\frac{m_0^2+m_1^2}{2}+\frac{m_0^2-m_1^2}{2\cos 2\theta}, \tag{16}$$

$$m_\rho^2=\frac{m_0^2+m_1^2}{2}-\frac{m_0^2-m_1^2}{2\cos 2\theta}, \tag{17}$$

are interpreted as the effective masses of ω and ρ^0 in neutron matter. When $n=0$, therefore, they reduce to their free values, that is, $m_\omega=782$ MeV and $m_\rho=770$ MeV. Note that there is a critical angle for which either m_ω^2 or m_ρ^2 can vanish. It actually takes place for m_ρ^2 when the mixing angle reaches θ_c defined by

$$\cos 2\theta_c=\left(\frac{m_\omega^2-m_\rho^2}{m_\omega^2+m_\rho^2}\right)_{n=0}\cos 2\theta_0, \tag{18}$$

where θ_0 is the mixing angle at $n=0$.

The nucleon field satisfies the Lagrange equation which is derived from Eq. (13):

$$[i\gamma^\mu\partial_\mu-M^*(\phi_c)]\Psi(x)=(g\omega_c+g'\tau_3\rho_c)\gamma^0\Psi(x). \tag{19}$$

This can be solved easily and the ground state of neutron matter can be constructed for a given neutron number density. The classical meson fields are obtained from

$$\phi_c=\frac{f}{m_\sigma^2}n_s, \tag{20}$$

$$\omega_c=\frac{g_n}{m_\omega^2}n, \tag{21}$$

$$\rho_c=-\frac{g'_n}{m_\rho^2}n, \tag{22}$$

in terms of the vector and scalar densities defined by

$$n=\langle:\Psi^\dagger\Psi:\rangle, \tag{23}$$

$$n_s=\langle:\bar{\Psi}\Psi:\rangle, \tag{24}$$

respectively. Here $:Q:$ represents the normal product of an operator Q. The right-hand side of Eq. (24) can be calculated to give

$$n_s=\frac{M_n^*}{2\pi^2}\left[KE_F-M_n^{*2}\ln\left(\frac{K+E_F}{M_n^*}\right)\right], \tag{25}$$

where K and $E_F=\sqrt{M_n^{*2}+K^2}$ are the Fermi momentum and energy of neutrons. Note that K is related to n by $K=(3\pi^2 n)^{1/3}$ which emerges from Eq. (23).

With the help of Eq. (25), we can transform Eqs. (9) and (20) into the coupled equations which determine the effective masses of proton and neutron in neutron matter:

$$M_b^*=M_b-\frac{f^2M_n^*}{2\pi^2m_\sigma^2}\left[KE_F-M_n^{*2}\ln\left(\frac{K+E_F}{M_n^*}\right)\right]. \tag{26}$$

The energy density and pressure of neutron matter can be obtained easily according to the usual procedures given in standard textbooks [13]:

$$\mathcal{E}=\frac{1}{8\pi^2}\left[KE_F(M_n^{*2}+2K^2)-M_n^{*4}\ln\frac{K+E_F}{M_n^*}\right] +\frac{m_\sigma^2}{2f^2}(M_n-M_n^*)^2+\frac{1}{2}\left(\frac{g_n^2}{m_\omega^2}+\frac{g_n'^2}{m_\rho^2}\right)n^2, \tag{27}$$

$$p=-\frac{1}{24\pi^2}\left[KE_F(3M_n^{*2}-2K^2)-3M_n^{*4}\ln\frac{K+E_F}{M_n^*}\right] -\frac{m_\sigma^2}{2f^2}(M_n-M_n^*)^2+\frac{1}{2}\left(\frac{g_n^2}{m_\omega^2}+\frac{g_n'^2}{m_\rho^2}\right)n^2. \tag{28}$$

Note that the density dependence of CSB appears through θ, and hence through g_n, g'_n, m_ω, and m_ρ.

III. ISOSPIN MIXING IN NEUTRON MATTER

Let us express $\epsilon(n)$, which determines the magnitude of the isospin mixing, in terms of the transition amplitude between the vector mesons in different isospin eigenstates in neutron matter. We follow the procedure that we used for the study of CSB in nuclear matter in our previous paper [10]. Here we give only the basic idea to obtain $\epsilon(n)$. We first construct the transition amplitude between the isoscalar- and isovector-vector mesons. Then we average it with an appropriate weight function. Finally we relate the averaged amplitude to $\epsilon(n)$. Since only the time component of the vector meson fields is relevant in the MFA, we consider the transition between the time component of the vector mesons.

Apart from trivial factors, the transition amplitude between the isoscalar- and isovector-vector mesons is given by

$$\mathcal{M}(k;n)=G_0\Pi^{(V)}(k;n)G_1+G_0\Pi^{(T)}(k;n)F_1, \qquad (29)$$

where

$$\Pi^{(V)}(k;n)=-i\int\frac{d^4p}{(2\pi)^4}\mathrm{Tr}[\gamma^0G(p+k)\gamma^0\tau_3G(p)], \qquad (30)$$

$$\Pi^{(T)}(k;n)=-i\int\frac{d^4p}{(2\pi)^4}\mathrm{Tr}\left[\gamma^0G(p+k)\times\left(\frac{-ik_\mu\sigma^{\mu0}}{2M_N}\right)\tau_3G(p)\right]. \qquad (31)$$

The first and second terms on the right-hand side in Eq. (29) represent the contributions from the baryon loops whose vertices with the isovector meson are subject to the vector and tensor couplings, respectively. The propagator $G(p)$ of nucleon with four-momentum p is a diagonal matrix in isospin space. The elements are given by

$$G_p(p)=\frac{\gamma P_p+M_p^*}{P_p^2-M_p^{*2}+i\epsilon}, \qquad (32)$$

$$G_n(p)=\frac{\gamma P_n+M_n^*}{P_n^2-M_n^{*2}+i\epsilon}+i\pi\frac{\gamma P_n+M_n^*}{E_n(\boldsymbol{p})}\delta\times[P_{n0}-E_n(\boldsymbol{p})]\theta(K-|\boldsymbol{p}|), \qquad (33)$$

for neutron matter, where $P_b^\mu=(P_{b0},\boldsymbol{p})$ and their time components are defined by

$$P_{p0}=p_0-\left(\frac{g_pg_n}{m_\omega^2}-\frac{g_p'g_n'}{m_\rho^2}\right)n, \qquad (34)$$

$$P_{n0}=p_0-\left(\frac{g_n^2}{m_\omega^2}+\frac{g_n'^2}{m_\rho^2}\right)n. \qquad (35)$$

We work in the static limit for nucleons. Then we can evaluate the integrals in Eqs. (30) and (31) analytically with the help of dimensional regularization. We obtain

$$\Pi^{(V)}(k;n)=\frac{k^2}{2\pi^2}\int_0^1dzz(1-z)\ln\left|\frac{M_p^{*2}+z(1-z)k^2}{M_n^{*2}+z(1-z)k^2}\right|+\frac{1}{4\pi^2k}\int_0^Kdpp\frac{4E_n^2(p)-k^2}{E_n(p)}\ln\left|\frac{2p+k}{2p-k}\right|+\frac{1}{2\pi^2}\left\{KE_F-M_n^{*2}\ln\left(\frac{K+E_F}{M_n^*}\right)\right\} \qquad (36)$$

for Eq. (30), where we denote $|\boldsymbol{k}|$ with k. Similarly we have

$$\Pi^{(T)}(k;n)=-\frac{k^2}{8\pi^2}\sum_b\eta_b\frac{M_b^*}{M_N}\int_0^1dz\ln|M_b^{*2}+z(1-z)k^2|+\frac{k}{4\pi^2}\frac{M_n^*}{M_N}\int_0^Kdp\frac{p}{E_n(p)}\ln\left|\frac{2p+k}{2p-k}\right| \qquad (37)$$

for Eq. (31), where $\eta_b=+1$ for $b=p$ and -1 for $b=n$.

As we have done in the previous paper, we incorporate the effect due to the multiple scattering of nucleons by the CSB interactions into $\epsilon(n)$. Considering that a wide range of momentum transfer is involved in the multiple scatterings, we take an appropriate average of $\mathcal{M}(k;n)$ with respect to the momentum k. Then we can relate the average which we denote with $\bar{\mathcal{M}}(n)$ to $\epsilon(n)$ by

$$\epsilon(n)=\epsilon_0\frac{\bar{\mathcal{M}}(n)}{\bar{\mathcal{M}}_0}, \qquad (38)$$

where $\bar{\mathcal{M}}_0\equiv\bar{\mathcal{M}}(n=0)$ and ϵ_0 is a parameter representing $\epsilon(n)$ at $n=0$.

For the weight function to obtain $\bar{\mathcal{M}}(n)$, we utilize the product of the form factors at the vertices associated with ω and ρ^0 in the Bonn potential. The normalized weight function is, therefore,

$$F(k)=\frac{1}{\pi^2}\frac{\Lambda_0\Lambda_1(\Lambda_0+\Lambda_1)^3}{(\Lambda_0^2+k^2)^2(\Lambda_1^2+k^2)^2}, \qquad (39)$$

where Λ_0 and Λ_1 are the cutoff momenta for the isoscalar- and isovector-vector mesons. We use the values used in the Bonn potential for Λ_0 and Λ_1, that is, $\Lambda_0=\Lambda_1\equiv\Lambda=1850$ MeV [17]. Then we have

$$\bar{\mathcal{M}}(n)=\int d^3kF(k)\mathcal{M}(k;n). \qquad (40)$$

The integration with respect to k can be performed analytically to give the averages of $\Pi^{(V)}(k;n)$ and $\Pi^{(T)}(k;n)$:

$$\overline{\Pi}^{(V)}(n)=\frac{\Lambda^2}{6\pi^2}\ln\left(\frac{M_p^*}{K+E_F}\right)+\frac{KE_F}{\pi^2}-\frac{\Lambda^2}{12\pi^2(\Lambda^2-4M_n^{*2})^2}\left[\frac{8KE_F}{\Lambda^2+4K^2}\left\{(\Lambda^2-4M_n^{*2})^2-4M_n^{*2}(\Lambda^2+2M_n^{*2})-\frac{4\Lambda^2M_n^{*2}(\Lambda^2-4M_n^{*2})}{\Lambda^2+4K^2}\right\}-\Lambda^2(\Lambda^2-10M_n^{*2})W(n)\right]+\frac{\Lambda^2}{6\pi^2}\sum_b\eta_b\frac{4M_b^{*2}(\Lambda^2+2M_b^{*2})+\Lambda^2(\Lambda^2-10M_b^{*2})Z(M_b^*)}{(\Lambda^2-4M_b^{*2})^2}, \tag{41}$$

$$\overline{\Pi}^{(T)}(n)=-\alpha\frac{\Lambda^2}{4\pi^2}\ln\left(\frac{M_p^*}{K+E_F}\right)+\alpha\frac{\Lambda^4}{24\pi^2(\Lambda^2-4M_n^{*2})^2}\left[\frac{16KE_F}{(\Lambda^2+4K^2)}\left\{\Lambda^2-10M_n^{*2}-\frac{\Lambda^2(\Lambda^2-4M_n^{*2})}{\Lambda^2+4K^2}\right\}-3(\Lambda^2-8M_n^{*2})W(n)\right]-\alpha\frac{\Lambda^2}{12\pi^2}\sum_b\eta_b\frac{4M_b^{*2}(\Lambda^2+8M_b^{*2})+3\Lambda^2(\Lambda^2-8M_b^{*2})Z(M_b^*)}{(\Lambda^2-4M_b^{*2})^2}, \tag{42}$$

where

$$W(n)=\frac{2\Lambda}{\sqrt{4M_n^{*2}-\Lambda^2}}\tan^{-1}\frac{K\sqrt{4M_n^{*2}-\Lambda^2}}{\Lambda E_F}\quad(2M_n^*>\Lambda)$$
$$=\frac{\Lambda}{\sqrt{\Lambda^2-4M_n^{*2}}}\ln\left|\frac{K\sqrt{\Lambda^2-4M_n^{*2}}+\Lambda E_F}{K\sqrt{\Lambda^2-4M_n^{*2}}-\Lambda E_F}\right|\quad(2M_n^*<\Lambda), \tag{43}$$

$$Z(x)=\frac{2\Lambda}{\sqrt{4x^2-\Lambda^2}}\tan^{-1}\sqrt{\frac{2x-\Lambda}{2x+\Lambda}}\quad(2x>\Lambda)$$
$$=\frac{\Lambda}{\sqrt{\Lambda^2-4x^2}}\ln\left|\frac{\sqrt{\Lambda+2x}+\sqrt{\Lambda-2x}}{\sqrt{\Lambda+2x}-\sqrt{\Lambda-2x}}\right|\quad(2x<\Lambda), \tag{44}$$

and $\alpha=(M_p^*+M_n^*)/(M_p+M_n)$. In obtaining Eq. (42), we replaced (M_p^*/M_N) and (M_n^*/M_N) with α in good approximation. For $n=0$, Eqs. (41) and (42) reduce to

$$\overline{\Pi}_0^{(V)}=\frac{\Lambda^2}{6\pi^2}\ln\left(\frac{M_p}{M_n}\right)+\frac{\Lambda^2}{6\pi^2}\sum_b\eta_b\frac{4M_b^2(\Lambda^2+2M_b^2)+\Lambda^2(\Lambda^2-10M_b^2)Z(M_b)}{(\Lambda^2-4M_b^2)^2}, \tag{45}$$

$$\overline{\Pi}_0^{(T)}=-\frac{\Lambda^2}{4\pi^2}\ln\left(\frac{M_p}{M_n}\right)-\frac{\Lambda^2}{12\pi^2}\sum_b\eta_b\frac{4M_b^2(\Lambda^2+8M_b^2)+3\Lambda^2(\Lambda^2-8M_b^2)Z(M_b)}{(\Lambda^2-4M_b^2)^2}. \tag{46}$$

Finally we obtain

$$\epsilon(n)=\epsilon_0\frac{\overline{\Pi}^{(V)}(n)+C_1\overline{\Pi}^{(T)}(n)}{\overline{\Pi}_0^{(V)}+C_1\overline{\Pi}_0^{(T)}}, \tag{47}$$

where $C_1=F_1/G_1$.

The parameter ϵ_0 is determined as follows. We fix θ_0 such that a nuclear force of which ω and ρ^0 are those defined by Eqs. (10) and (11) reproduces a quantity attributed to CSB. Actually, when we choose $\theta_0=4°$ and use g and g' for the coupling constants of ω and ρ^0 with the nucleon, the Bonn potential reproduces the difference between the nn and Coulomb corrected pp scattering lengths. Then the observed masses of ω and ρ^0 determine m_0 and m_1 through Eqs. (16) and (17), and ϵ_0 is obtained from Eq. (12) with $\theta=\theta_0$.

IV. CALCULATIONS AND DISCUSSIONS

In the present study we are interested in (i) the nuclear density dependence of the mixing angle and (ii) the influence of DDCSB on the equation of state of neutron matter. When we compare our results with those emerging from ordinary nuclear models, we refer to the QHD II as a typical one of ordinary models. To be consistent, therefore, we fix the meson-nucleon coupling constants appearing in the present calculations to the values used in QHD II [13]:

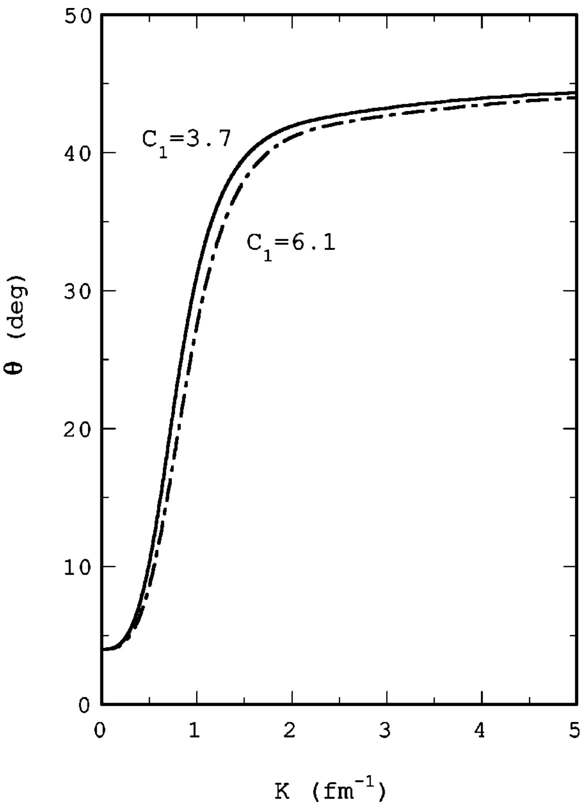

FIG. 1. Density dependence of the isospin mixing angle. The solid and dot-dashed curves correspond to $C_1 = 3.7$ and 6.1, respectively. When $K=0$, θ goes to 4°. The θ approaches to 44.6° in the high density limit.

$$f^2\left(\frac{M_N}{m_\sigma}\right)^2 = 267.1, \tag{48}$$

$$G_0^2\left(\frac{M_N}{m_0}\right)^2 = 195.9,$$

$$G_1^2\left(\frac{M_N}{m_1}\right)^2 = \frac{54.71}{4}.$$

Note that the numerical factor of 4 on the right-hand side of the third relation is due to the difference of our definition of the isovector interaction in Eq. (1) from the definition in Ref. [13]. The tensor coupling constant F_1 is somewhat ambiguous, lying in the interval from $C_1 = F_1/G_1 = 3.7$ to 6.1 [15]. We perform our calculations for both extrema of F_1.

First of all, we calculate θ which is obtained from Eq. (12) with Eq. (47). The density dependence of θ is shown in Fig. 1. One can see that the isospin mixing is very much and rapidly enhanced as the neutron density increases. It reaches 41° (40°) already at $n = 0.17$ fm^{-3}, the normal density of nuclear matter, when $C_1 = 3.7$ (6.1). This is in contrast to $\theta = 2°$, a small suppression of CSB, for nuclear matter with normal density [10]. We emphasize that our specific choice of nuclear model has nothing to do with the enhancement of CSB due to the large isospin mixing, but the medium effect is essential for it.

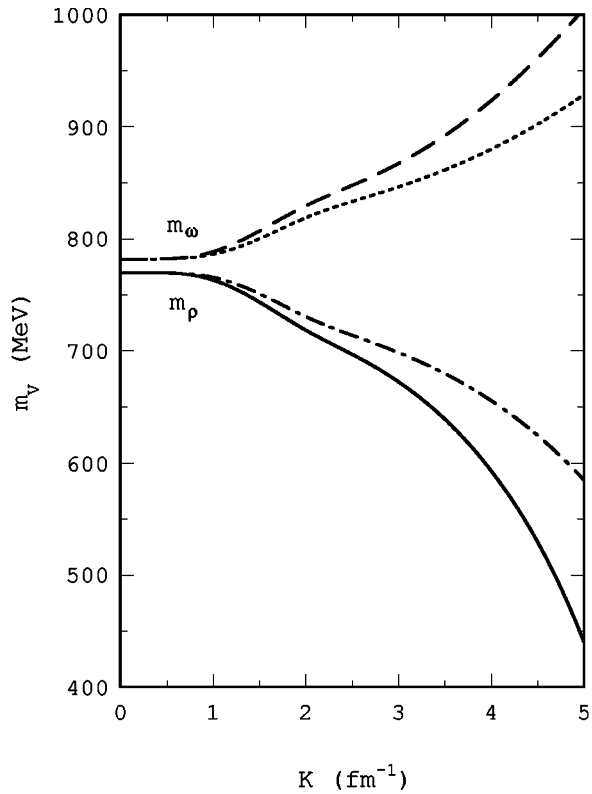

FIG. 2. Masses of physical vector mesons in neutron matter. The solid and dot-dashed curves represent the masses of ρ^0 with $C_1 = 3.7$ and 6.1, respectively, and the long-dashed and dotted curves the masses of ω with $C_1 = 3.7$ and 6.1, respectively. At densities higher than $K = 5.9$ (7.3) fm^{-1} for $C_1 = 3.7$ (6.1), m_ρ^2 dives into negative values.

The effective masses of vector mesons are also modified to a large extent. According to Eqs. (16) and (17), we can calculate m_ω and m_ρ for a given neutron density. The result is depicted in Fig. 2, showing a large modification of them. As we have mentioned in the preceding section, it is not surprising that the system described by $\mathcal{L}_{MFT}$ becomes unstable with respect to the excitation of the ρ degree of freedom. The critical density to give $m_\rho^2 = 0$ is $n_c = 6.90$ fm^{-3} for $C_1 = 3.7$, and the critical mixing angle is $\theta_c = 44.6°$ which we can obtain from Eq. (18). However, this instability should not be understood as such caused by a *quantum* excitation with ρ quantum number in neutron matter, since quantum fluctuation which is coupled with nuclear excitation has been ignored throughout in the MFA. In addition, it occurs at an extremely high density region where nucleons will no longer be the only relevant degree of freedom. It is interesting to see whether or not such a ρ instability is generated by DDCSB in neutron matter when the quantum fluctuation is taken into account. We leave this for a later investigation. When we study the effects of DDCSB on various quantities in the framework of the MFA, we shall not proceed with our calculations exceeding $n = 6.90$ fm^{-3} hereafter. Note that this value of n is considerably larger than the central density of a neutron star with its heaviest mass.

The energy per nucleon, which is defined by

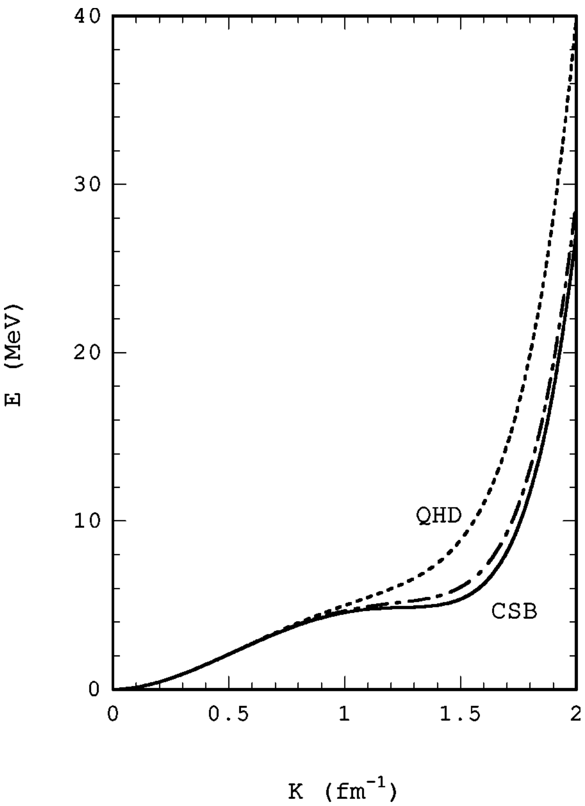

FIG. 3. The energy per nucleon as a function of the Fermi momentum. The solid and dot-dashed curves show the energies obtained from the model with DDCSB with $C_1 = 3.7$ and 6.1, respectively, and the dotted curve the energy from QHD II.

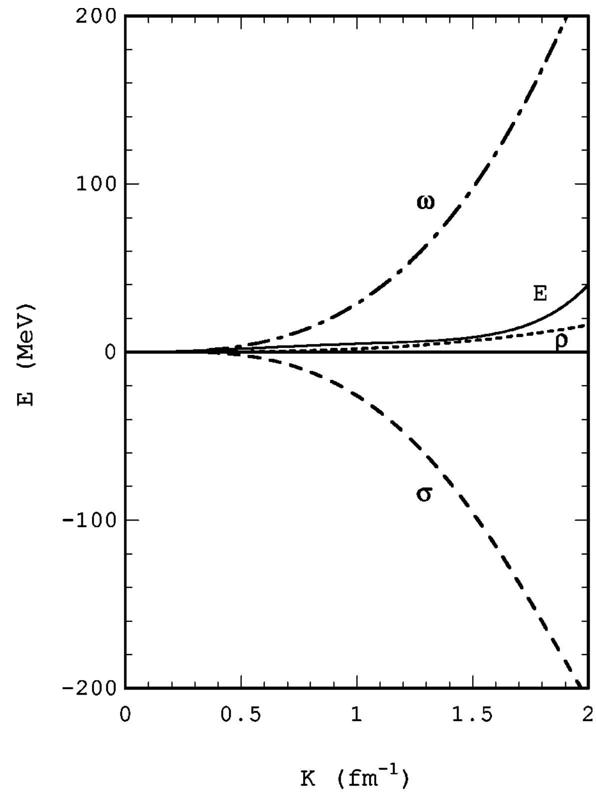

FIG. 4. Contributions from individual meson degrees of freedom on the right-hand side of Eq. (27) to E obtained from QHD II. The long-dashed, dot-dashed, and dotted curves represent the contributions from σ, ω, and ρ. The solid curve represents the sum of them.

$$E = \frac{\mathcal{E}}{n} - M_n, \tag{49}$$

is depicted in Fig. 3 as a function of the Fermi momentum. The solid and dot-dashed curves represent the energies which we obtain from the model with DDCSB with $C_1 = 3.7$ and 6.1, respectively, and the dotted curve the one from QHD II. We show the contributions from individual meson degrees of freedom in Eq. (27) to E in Figs. 4 and 5 for QHD II and the model with DDCSB, respectively. The first term of Eq. (27) contains an attractive interaction of σ with nucleons. The σ-field energy, the second term in Eq. (27), is positive and smaller than the attractive interaction energy with nucleons in magnitude. Thus the energy per nucleon arising from the σ degree of freedom, which is drawn with the long-dashed curves in the figures, turns out to be negative when they are added. In QHD II, therefore, ω is responsible for most of the repulsive interaction with nucleons in neutron matter. On the other hand, our calculation with DDCSB shows that the repulsive interaction of ω with nucleons is suppressed by the enhancement of CSB, while the repulsive interaction of ρ develops as neutron density increases. The plateau behavior seen in the energy obtained from the model with DDCSB in Fig. 3 arises essentially from suppression of the repulsive interaction of ω with nucleons.

The pressure obtained from Eq. (27) is shown in Fig. 6 as a function of logarithmic neutron density. It is seen that neutron matter with DDCSB is softer around $\rho = 10^{14} \sim 10^{15}$ g/cm^3 ($n = 0.06 - 0.60$ fm^{-3}) than that described by QHD II. Interestingly the central densities with which neutron stars can be formed in a supernova explosion fall into this interval. Let us demonstrate how large the effect of DDCSB appears on bulk quantities by calculating the mass of a fictitious neutron star which is assumed to be in the ground state of a nuclear system composed of only neutrons. Our neutron star can approximate actual neutron stars with central densities around or higher than the normal density of nuclear matter, $\rho_{NM} = 2.84 \times 10^{14}$ g/cm^3. As discussed by Pethick and Ravenhall, when actual neutron stars have central densities lower than ρ_{NM}, they are likely to have crustal structure [19]. Also actual neutron stars contain electrons, protons, and other hadrons in addition to neutrons, being at beta equilibrium among them. Nevertheless, in order to illustrate the magnitude of DDCSB, it is still meaningful to evaluate the mass of such a fictitious neutron star. The mass is obtained by applying Eq. (27) to the Tolman-Oppenheimer-Volkoff equation [18]. We compare our results with those emerging from QHD II with no CSB considered and see the effect under a common scheme of relativistic many-body theories. The result is depicted in Fig. 7 as a function of the central density. Since the nuclear force with

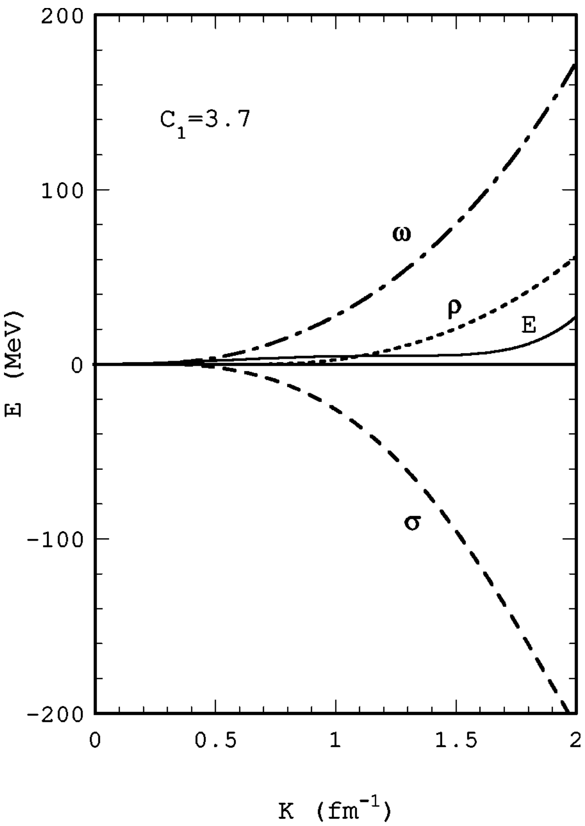

FIG. 5. Contributions from individual meson degrees of freedom on the right-hand side of Eq. (27) to E obtained from the model with DDCSB. The result with $C_1=3.7$ is shown. The attributes of curves are the same as those in Fig. 4.

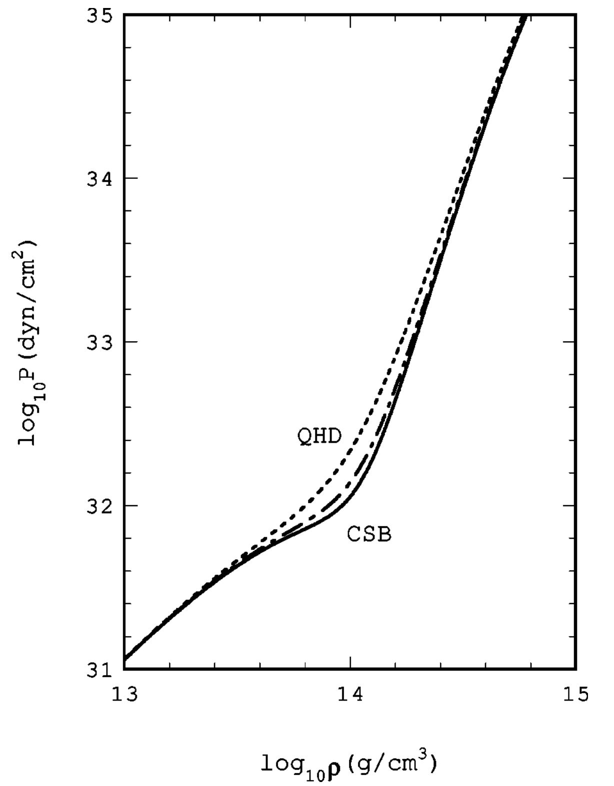

FIG. 6. The pressure vs density. The solid and dot-dashed curves represent the pressures emerging from the calculations with $C_1=3.7$ and 6.1, respectively, and the dotted curve the pressure from QHD II.

DDCSB yields a softer equation of state than the one which ordinary nuclear forces do, naturally DDCSB works to reduce the masses from those which QHD II predicts. Reduction amounts to approximately 35% for stars with central densities around ρ_{NM}. The effect due to DDCSB is attenuated for the stars with higher central densities which actual neutron stars are supposed to have. We will study separately whether or not it remains to be reckoned with.

We do not proceed with further calculations for neutron stars. But let us speculate about what takes place in actual neutron stars when the charge symmetry of the nuclear force is strongly broken inside the stars. We have seen that the strong enhancement of CSB leads to giving lower energy to neutron matter than ordinary nuclear forces do. It implies that actual neutron stars will enhance CSB and, hence, will reduce the energy by transferring a number of protons to neutrons. Thus neutron stars will contain a smaller number of protons than ordinary nuclear forces predict. Consequently the Urca process will be suppressed and the cooling of neutron stars will be decelerated [20].

To summarize, we have investigated DDCSB due to the isospin mixing between isoscalar- and isovector-vector mesons in neutron matter. It was found that isospin mixing is rapidly and strongly enhanced as the neutron density increases. Consequently the charge symmetry is broken to a large extent. We saw that DDCSB modifies the energy per

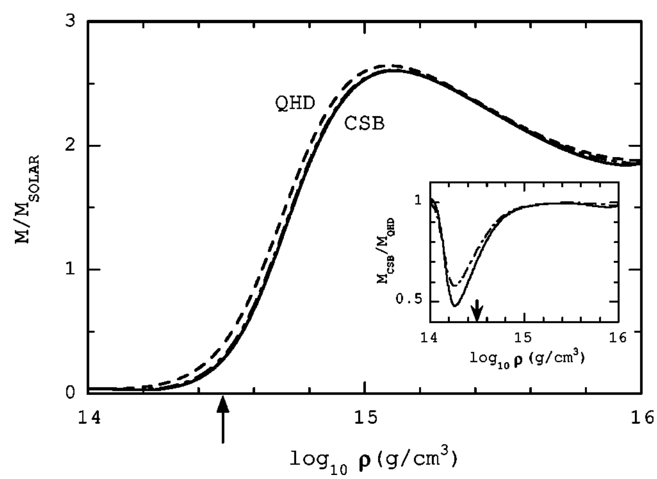

FIG. 7. The mass of the neutron star vs the central density. The solid and dot-dashed curves labeled as CSB are the masses emerging from the model with DDCSB with $C_1=3.7$ and 6.1, respectively, and the dotted curve labeled as QHD is the mass from QHD II. The solar mass is denoted by $M_{\rm solar}$. The inset shows the ratio of the masses emerging from the model with DDCSB and QHD II, where the solid curve corresponds to the case with $C_1=3.7$ and the dot-dashed curve to the case with $C_1=6.1$. The vertical arrows in the large and small figures indicate the neutron density corresponding to the normal density of nuclear matter, $\rho_{NM}=2.84\times10^{14}$ g/cm^3.

nucleon and the equation of state in neutron matter. As a demonstration of DDCSB, we showed that the masses of fictitious neutron stars composed of only neutrons are decreased by a sizable amount in comparison with those emerging from the ordinary nuclear model with no CSB considered. This demonstration warns us that, unless one takes DDCSB into account, one cannot apply ordinary nuclear forces to a nuclear system with large isospin asymmetry such as unstable nuclei with large neutron excess.

ACKNOWLEDGMENTS

One of the authors (A.S.) would like to express his sincere thanks to Professor T. Udagawa and colleagues at the University of Texas at Austin for their warm hospitality and many useful discussions during his stay in 1998. He also would like to thank Yuki Nogami and colleagues at the McMaster University for fruitful discussions and their warm hospitality extended to him during his stay in 1998.

[1] E. M. Henley and G. A. Miller, in *Mesons in Nuclei*, edited by M. Rho and D. Wilkinson (North-Holland, Amsterdam, 1979), Vol. III, p. 495; G. A. Miller and W. T. H. van Oers, in *Symmetries and Fundamental Interactions in Nuclei*, edited by W. C. Haxton and E. M. Henley (World Scientific, Singapore, 1995), p. 127, and all references quoted therein.
[2] P. G. Blunden and M. J. Iqbal, Phys. Lett. B **198**, 144 (1987).
[3] O. Schori *et al.*, Phys. Rev. C **35**, 2252 (1987).
[4] W. von Witsch, B. Gomez Moreno, W. Rosenstock, K. Ettling, and J. Bruinsma, Phys. Lett. **80B**, 187 (1979); Nucl. Phys. **A329**, 141 (1979).
[5] K. Okamoto, Prog. Theor. Phys. **19**, 471 (1969).
[6] S. A. Coon and R. C. Barrett, Phys. Rev. C **36**, 2189 (1987).
[7] G. A. Miller, B. M. K. Nefkens, and L. Slaus, Phys. Rep. **194**, 1 (1990).
[8] Y. Nogami and Y. P. Varshni, Nuovo Cimento **25**, 218 (1962); B. W. Downs and Y. Nogami, Nucl. Phys. **B2**, 459 (1967).
[9] J. Piekarewicz and A. G. Williams, Phys. Rev. C **47**, R2462 (1993).
[10] M. Kimura, A. Suzuki, and H. Tezuka, Phys. Lett. B **367**, 5 (1996); M. Kimura, A. Suzuki, K. Suzuki, and H. Tezuka, Phys. Rev. C **56**, 3070 (1997).
[11] J. A. Nolen and J. P. Schiffer, Annu. Rev. Nucl. Sci. **19**, 471 (1969).
[12] J. Zimanyi and S. A. Moszkowski, Phys. Rev. C **42**, 1416 (1990).
[13] J. D. Walecka, Ann. Phys. (N.Y.) **83**, 491 (1974); B. D. Serot and J. D. Walecka, Adv. Nucl. Phys. **16**, 1 (1986); J. D. Walecka, *Theoretical Nuclear and Subnuclear Physics* (Oxford University Press, New York, 1995).
[14] J. D. Bjorken and S. D. Drell, *Relativistic Quantum Mechanics* (McGraw-Hill, New York, 1964).
[15] A. C. Davis, W. N. Cottingham, and J. W. Alock, Nucl. Phys. **B111**, 233 (1976).
[16] S. A. Chin and J. D. Walecka, Phys. Lett. **52B**, 24 (1974); S. A. Chin, Ann. Phys. (N.Y.) **108**, 301 (1977); R. Brockmann and J. Frank, Phys. Rev. Lett. **68**, 1830 (1992).
[17] R. Machleidt, K. Holinde, and Ch. Elster, Phys. Rep. **149**, 1 (1987).
[18] J. R. Oppenheimer and G. M. Volkoff, Phys. Rev. **55**, 374 (1939).
[19] C. J. Pethick and D. G. Ravenhall, Annu. Rev. Nucl. Part. Sci. **45**, 429 (1995).
[20] C. J. Pethick, Rev. Mod. Phys. **64**, 1133 (1992).